

Film growth of germanium on Ru(0001) studies by scanning tunneling microscopy

H. J. Zhang,¹ B. Lu,¹ X.-S. Wang,² F. Hu,¹ H. Y. Li,¹ S. N. Bao,¹ and P. He^{1,*}

¹Department of Physics, Zhejiang University, Hangzhou, 310027, China

²Department of Physics, National University of Singapore, Lower Kent Ridge Road, Singapore 119260

(Received 24 June 2004; revised manuscript received 8 September 2004; published 14 December 2004)

Using *in situ* scanning tunneling microscopy, we observed that germanium deposited on the Ru(0001) surface near room temperature forms a two-dimensional wetting layer in the submonolayer regime, followed with growth of a segregated layer of Ge three-dimensional (3D) clusters of heights within about 1 nm. The growth of the first flat wetting layer can be understood in terms of optimal surface energy reduction by coating the Ru surface with a Ge layer which has a lower surface free energy. The nucleation and growth kinetics agrees with that derived from the conservative Ising model. Domains of a $(\sqrt{21} \times \sqrt{21})R10.9^\circ$ superstructure are observed on the wetting layer. Formation of a layer consisting of 1-nm-high clusters above the wetting layer indicates that the Ge wetting layer is extremely inert so that Ge adatoms can migrate large distances on the top of the wetting layer. The 3D Ge clusters seem to have a relatively narrow size distribution.

DOI: 10.1103/PhysRevB.70.235415

PACS number(s): 68.35.Bs, 81.15.Hi, 68.37.Ef

I. Introduction

Film growth and interface behavior of metals on semiconductor surfaces have been intensively explored in the past,¹⁻⁴ whereas there are only a few studies on the reverse systems, i.e., semiconductors on metal surfaces.⁵⁻¹⁰ Such systems also involve fundamental issues, such as growth mechanism, novel surface electronic structures, and formation of surface alloy/compound. Understanding of these issues is helpful to the applications of these systems in catalysis^{11,12} and possibly electronics in the future. On the (111) surfaces of noble metals (Cu and Ag),^{5,7} a submonolayer of Ge deposited at room temperature forms surface alloy layers through replacement reaction, while Ge stays on (100) surfaces of these metals as adsorbed atoms or clusters.⁸ On Pt(111), a (5×5) dilute surface alloy is formed after 2 monolayer (ML) Ge deposition followed with a 1300 K annealing.⁹ On Pt(100), Ge expels Pt adatoms and the expelled atoms form pure Pt adislands. It is difficult to predict general behavior of semiconductor materials deposited on metals based on the very limited experimental data available now.

In this paper, we report on our scanning tunneling microscopy (STM) investigations of germanium growth on the Ru(0001) surface. Ru is a transition metal with a hexagonal close packed (HCP) lattice structure. The Ge/Ru system can be considered as a model system for well understanding growth behavior of semiconductors on HCP metal surfaces. RuGe and Ru₂Ge₃ can be formed in bulk phase.¹³ Ru₂Ge₃ is a semiconductor, with a band gap in the range of 0.31–0.85 eV obtained in computation studies.^{14,15} To the best of our knowledge, initial reaction and growth of Ge on Ru(0001) has not been reported. Our results show that Ge forms a wetting layer first in the monolayer regime which is inert with respect to Ge atoms deposited later. A $(\sqrt{21} \times \sqrt{21})R10.9^\circ$ superstructure is observed on this wetting layer. Further Ge deposition leads to the growth of a cluster layer with a thickness of about 1 nm.

II. Experiment

The experiments were performed in a multifunctional ultrahigh-vacuum (UHV) VT-SPM system (Omicron) with a

base pressure better than 1×10^{-10} Torr. The system is described in detail elsewhere.^{16,17} In brief, in addition to a STM, it consists of a fast-entry lock for sample and tip loading, a preparation chamber, an analysis chamber, and an STM chamber. The system is equipped with resistive-heating Ta-boat Ge evaporators, an electron-bombardment sample heater, an argon-ion sputter gun, low-energy electron diffraction (LEED) optics, and an x-ray photoemission spectrometer (XPS).

The cleaning of the Ru(0001) surface was achieved by several circles of Ar⁺ sputtering and annealing, and

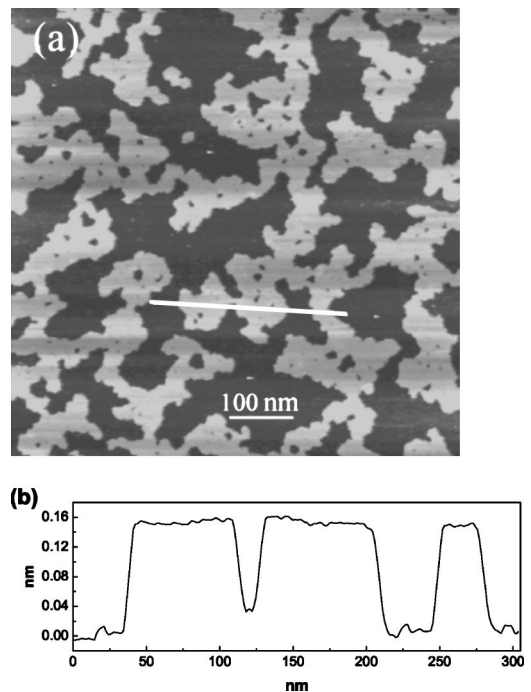


FIG. 1. (a) STM image ($500 \times 500 \text{ nm}^2$) of Ge on Ru(0001) at a coverage of 0.4 ML taken at sample bias $V_S = -0.41 \text{ V}$ and tunneling current $I_T = 0.10 \text{ nA}$. (b) The line profile along the line indicated in the STM image.

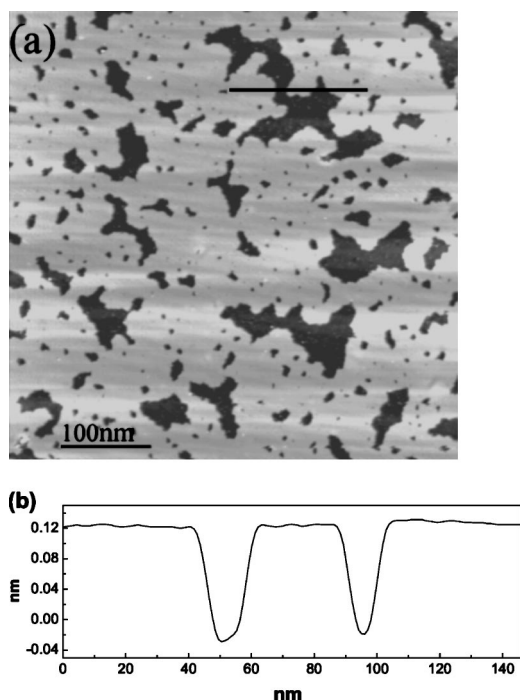


FIG. 2. (a) STM image ($500 \times 500 \text{ nm}^2$) of Ge on Ru(0001) at a coverage of 0.8 ML taken at $V_S = -0.95 \text{ V}$ and $I_T = 0.15 \text{ nA}$. (b) The line profile along the line as indicated in the STM image.

the sample cleanliness was verified by LEED and XPS measurement. The Ta-boat Ge source was cleaned thoroughly with preheating, and the deposition was done at a source temperature of about 1200 K with a deposition rate of about 0.4 ML/min. Considering the heating effect of Ge source, the substrate temperature is estimated in the range of 40–60 °C during the Ge deposition.

III. Results and Discussion

Figs. 1 and 2 show the typical STM images (area $500 \times 500 \text{ nm}^2$) of Ru(0001) taken at the Ge coverage of about 0.4 and 0.8 ML, respectively. The Ge overlayer appears as the bright areas in the images. Based on the line profile [Fig. 1(b)] along the white line in Fig. 1(a), the Ge overlayer in the submonolayer regime is composed of single atomic layer islands with a thickness of about 1.5 Å. The Ge coverage estimated from the bright regions in the STM images is consistent with the deposited amounts of 0.4 and 0.8 monolayers.

The results clearly showed that, with the flux used in our experiment, the growth of Ge on Ru(0001) in the submonolayer regime proceeds strictly in the single layer growth mode, i.e., no second-layer nucleation and growth are observed. Thermodynamically, this is understandable considering the surface and interface energies in film growth.¹⁸ A smaller surface free energy of the overlayer and a strong overlayer-substrate binding lead to the first atomic layer coating the whole surface (wetting layer) to provide optimum energy reduction. The surface free energy of Ge is 1.1 J m^{-2} , which is significantly smaller than the Ru sub-

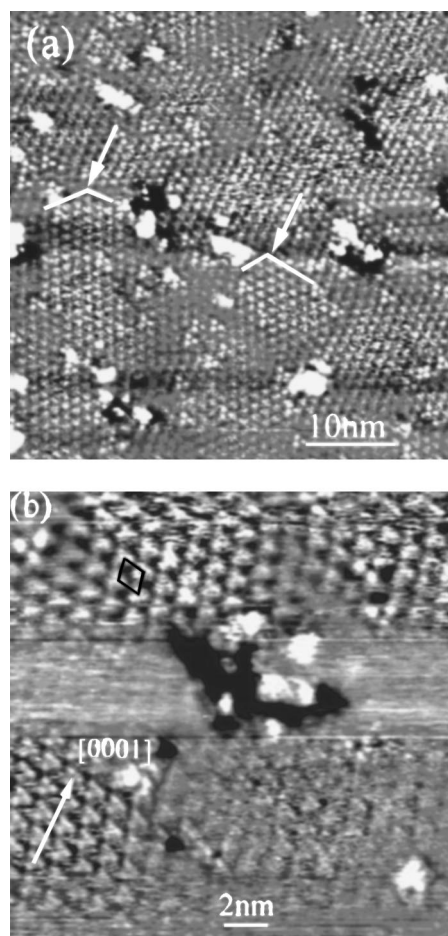


FIG. 3. (a) STM image ($49 \times 49 \text{ nm}^2$) of the $(\sqrt{21} \times \sqrt{21})R10.9^\circ$ superstructure on Ge wetting layer, the domain boundaries are indicated by the arrows. (b) A zoom-in image ($21 \times 21 \text{ nm}^2$) showing details of the superstructure, the unit cell of $(\sqrt{21} \times \sqrt{21})R10.9^\circ$ is indicated. Both images were taken with $V_S = 2.1 \text{ V}$ and $I_T = 0.15 \text{ nA}$.

strate surface free energy of 3.4 J m^{-2} .¹⁸ On the other hand, diffusion and nucleation kinetics of Ge atoms play an important role in determining the morphology and 2D island shape of the overlayer.^{19,20} For example, formation of fractal islands is typical for diffusion limited aggregation (DLA)^{21,22} growth in which diffusion of an individual atom on both substrate and island terraces is activated whereas atomic migration along an island edge is prohibited. If edge diffusion is also highly activated, the island shape should be compact. In the present case, the islands are neither fractal nor very compact. This indicates that the diffusivity of Ge atoms on Ru substrate is fairly high. The critical nucleus size of Ge islands is significantly larger than one atom so that nucleation density is relatively low (notice that empty areas of linear size $\sim 100 \text{ nm}$ are easily found in Fig. 1). As compared with that on a Ge crystal surface at comparable temperature,²³ the diffusion of Ge atoms on the Ru-supported Ge islands is also highly activated and the Ehrlich-Schwoebel barrier is little, so that the Ge atoms that landed on Ge islands can migrate over a long distance and cross the steps to settle at the lower edge of the Ge islands. But Ge

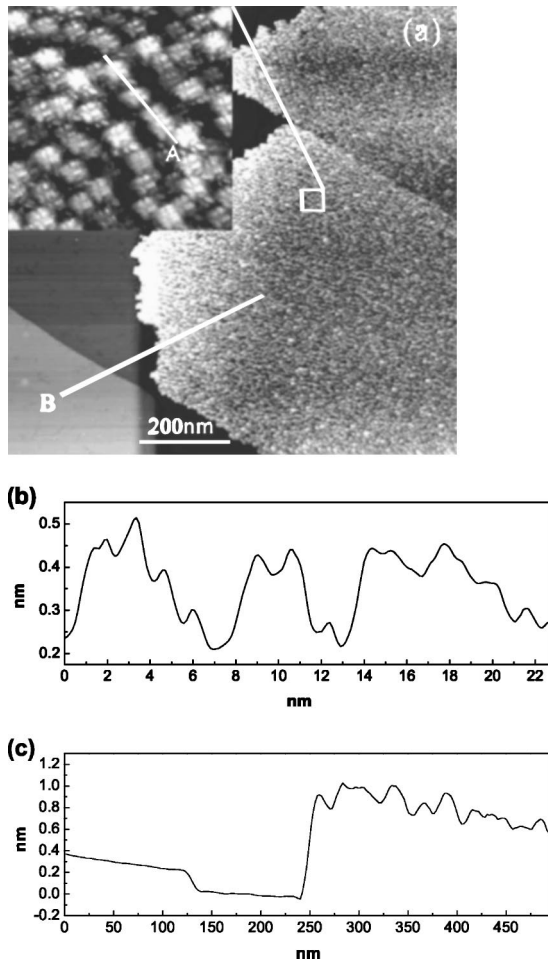


FIG. 4. (a) STM image ($1000 \times 1000 \text{ nm}^2$) of Ge on Ru(0001) at a nominal coverage of 1.6 ML, taken at $V_S=0.70 \text{ V}$ and $I_T=0.10 \text{ nA}$. The right region is a 1-nm-high layer composed of Ge clusters on the top of the wetting layer. The inset image, and the line profiles (b) along line A in the cluster region and (c) along line B across the edge of the cluster layer as indicated in the images show more details of the cluster layer.

island morphology is fractal-like on a large scale, similar to the Si/Si(111) case observed by Olami *et al.*²⁴ Such island morphology can be generated with a conservative Ising model in which an atom is allowed to migrate to a neighboring site after arriving at step edge.²⁴

On smaller scales, our STM images reveal an ordered superstructure on the Ge wetting layer surface. Figure 3(a) displays an image consisting of domains of periodic structures. The measured period of the ordered structure is 12.4 \AA or $4.6a_0$, where $a_0=2.706 \text{ \AA}$ is the length of basis on Ru(0001). The domains are rotated between each other by an angle $\sim 21.8^\circ$. Considering measurement error due to drift, the superstructure is assigned as $(\sqrt{21} \times \sqrt{21})R10.9^\circ$. More details of the $(\sqrt{21} \times \sqrt{21})R10.9^\circ$ superstructure can be observed in the zoom-in STM scan of Fig. 3(b). The supercell appears as an equilateral triangle with three bright spots at the apexes.

Figure 4(a) shows a STM image taken after a 1.6 ML Ge overlayer deposited near room temperature. The results indicate the growth of a layer of 3D clusters on top of the wet-

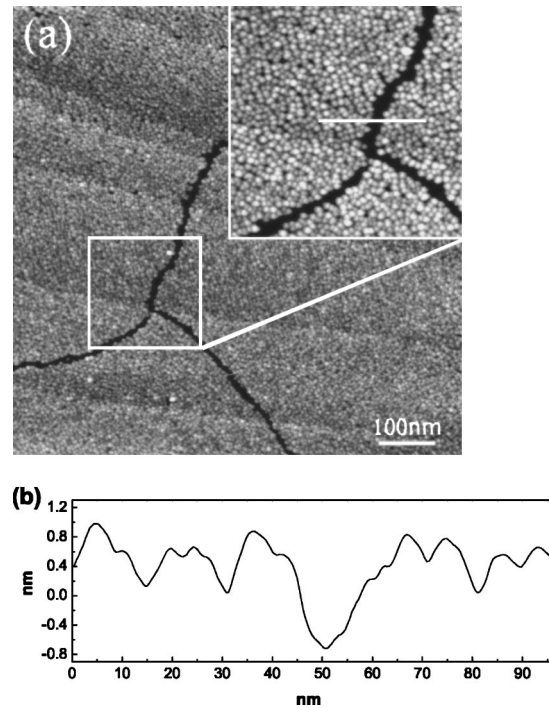


FIG. 5. (a) STM image ($780 \times 780 \text{ nm}^2$) of Ge on Ru(0001) at a nominal coverage of 4.0 ML, taken at $V_S=2.57 \text{ V}$ and $I_T=0.56 \text{ nA}$, shows the cracks formed due to strain release. (b) The line profile across a crack as indicated in (a).

ting layer. The line profiles on and across the edge of the cluster layer are displayed as line A and line B, respectively. The thickness of the cluster layer is approximately 1 nm. The corrugation observed on the layer is within about 0.4 nm, probably limited by tip sharpness, and the lateral dimension of the clusters is about 1.8 nm.

It should be noted that the local coverage in the 3D clusters is highly segregated, and most of the surface is only covered by the wetting layer. Actually, we had difficulty in STM imaging to find the cluster region shown in Fig. 4. Interestingly, once a cluster layer is found, its area is huge and can run across several atomic steps of the Ru substrate. This means that Ge adatoms or/and clusters are very mobile on the top of the Ge wetting layer. The Ge nucleation on top of the wetting layer only happens when Ge adatoms meet defects, for example, the steps. Ge adatoms on the top of the wetting layer can migrate (diffuse) over a large distance, once they meet with the 3D segregated clusters, they are cooperated into the clusters.

Figure 5 shows STM images for the Ge overlayer with a nominal coverage of about 4 ML. Compared with the results shown in Fig. 4, the only difference is that the 3D clusters become larger (the clusters with a layer thickness of about 1.4 nm, and a lateral dimension of about 5.0 nm, see the line profile across the rift in Fig. 5), and the rift appears by releasing the strain of the overlayer on Ru(0001).

By summarizing the above results for Ge growth on Ru(0001) from submonolayer to multilayer, we can conclude that Ge growth on Ru(0001) exhibits a Stranski-Krastanov (SK) mode, i.e., formation of 3D clusters on the top of a flat first (wetting) layer. However, the Ge clusters are largely

segregated due to their high mobility on the wetting layer, and it seems that the clusters have a uniform distribution. The Ge/Ru(0001) growth shows some unique characteristics compared to other SK growth systems, such as Ge on silicon.

Growth behavior of Ge/Si systems is well understood.²³ Ge grows on Si(001) in layer-by-layer mode up to ~ 3 ML, and the surface superstructure changes from (2×1) to $(2 \times N)$. When more Ge is deposited, coherent pyramids and huts are formed to partially release the mismatch strain.²⁵ On Si(111), a 3-ML Ge wetting layer is also formed first, followed with hexagon-shaped 3D islands.²⁶ The main driving force of SK growth in Ge/Si systems is to reduce strain energy due to lattice mismatch, and the 3D islands formed are epitaxial. In contrast, in the case of Ge growth on Ru(0001), Ge forms only a single atomic wetting layer, and grows in the 3D clusters mode on the top of the first wetting layer. The difference should arise from a different driving force due to the nature of the Ge wetting layer. Surface free energy should be the dominant factor for forming a single atomic wetting layer in Ge growth on Ru(0001). The lattice mismatch between Ge and Ru is about 10%. But it seems that the main reason for the 3D Ge cluster formation on the top of the wetting layer is not mismatch. Rather, the wetting layer seems to passivate the Ru surface very effectively, so the deposited Ge later experiences an inert surface. In other words, the surface of the Ge wetting layer on Ru(0001) is totally different in terms of bonding with the Ge deposited later, whereas the Ge wetting layers on Si are basically the same as the surfaces of bulk Ge crystal, except the strain due to the lattice mismatch with Si. Intermixing or alloying of Ge–Ru is not observed in the present (room temperature) growth condition. In comparison, Ge–Pt surface alloy was

obtained by deposition of 2 monolayers of Ge followed by heating to 1300 K in the system of Ge/Pt(111).⁹ We have also observed surface alloying of Ge on Ru(0001) after a high temperature annealing, which will be reported in detail elsewhere.

IV. Conclusion

We have carried out STM measurements for Ge growth on the Ru(0001) surface from submonolayer to multilayer. The results show clearly Ge growth on Ru(0001) exhibits a Stranski-Krastanov mode. Ge forms the two-dimensional wetting layer in the submonolayer regime and starts to grow in the 3D clusters mode from the second layer. The growth of the first flat wetting layer can be understood in terms of optimum energy reduction for Ge coating the whole substrate surface with smaller free surface energy. Formation of the segregated clusters from the second layer indicates that Ge adatoms can migrate large distances on the top of the first atomic layer. The Ge wetting layer on Ru(0001) appears extremely inert to the Ge atoms that land on it. The Ge clusters in the segregated layer seem to have a relatively narrow size distribution.

ACKNOWLEDGMENTS

This work has been supported by the National Natural Science Foundation of China under Grant No. 10274072, the Specialized Research Fund for the Doctoral Program of Higher Education of China under Grant No. 20030335017, and by the Agency for Science, Technology And Research (A*STAR) of Singapore (Project No. 012 101 0129).

*Corresponding author.

Electronic address: phypmhe@dial.zju.edu.cn

¹H. von Kaenel, *Mater. Sci. Rep.* **8**, 193 (1992).

²L. Floreano, D. Cvetko, F. Bruno, G. Bavdek, A. Cassaro, R. Gotter, A. Verdini, and A. Morgante, *Prog. Surf. Sci.* **72**, 135 (2003).

³M. Hammar, M. Goethelid, U. O. Karlsson, and S. A. Flodstrom, *Phys. Rev. B* **47**, 15 669 (1993).

⁴C. Collazo-Davila, D. Grozea, L. D. Marks, R. Feidenhans'l, M. Nielsen, L. Seehofer, L. Lottermoser, G. Falkenberg, R. L. Johnson, M. Goethelid, and U. Karsson, *Surf. Sci.* **418**, 395 (1998).

⁵R. Dudde, H. Bernhoff, and B. Reil, *Phys. Rev. B* **41**, 12 029 (1990).

⁶J. A. Martín-Gago, R. Fasel, J. Hayoz, R. G. Agostino, D. Naumović, P. Aebi, and L. Schlapbach, *Phys. Rev. B* **55**, 12 896 (1997); C. Polop, J. L. Sacedón, and J. A. Martín-Gago, *Surf. Sci.* **402**, 245 (1998).

⁷H. Oughaddou, S. Sawaya, J. Goniakowski, B. Aufray, G. Le Lay, J. M. Gay, G. Tréglia, J. P. Bibérian, N. Barrett, C. Guillot, A. Mayne, and G. Dujardin, *Phys. Rev. B* **62**, 16 653 (2000).

⁸H. Oughaddou, J. M. Gay, B. Aufray, L. Lepena, G. Le Lay, O.

Bunk, G. Falkenberg, J. H. Zeysing, and R. L. Johnson, *Phys. Rev. B* **61**, 5692 (2000).

⁹K. Fukutani, Y. Murata, J. Brillo, H. Kuhlenbek, H. J. Frund, and M. Taguchi, *Surf. Sci.* **464**, 48 (2000).

¹⁰M. Batzill, T. Matsumoto, C.-S. Ho, and B. E. Koel, *Phys. Rev. B* **69**, 113401 (2004).

¹¹K. Fukutani, T. T. Magekoev, Y. Murata, and K. Terakura, *Surf. Sci.* **363**, 185 (1996).

¹²T. Komatsu, M. Mesuda, and T. Yashima, *Appl. Catal., A* **194**, 333 (2000).

¹³P. Villars and X. Calvert, *Pearson's Handbook of Crystallographic Data for Intermetallic Phases* (American Society for Metals, Metals Park, OH, 1985), Vol. 3.

¹⁴A. B. Filonov, D. B. Migas, V. L. Shaposhnikov, V. E. Borisenko, and A. Heinrich, *Microelectron. Eng.* **50**, 249 (2000).

¹⁵W. Henrion, M. Rebien, A. G. Birdwell, V. N. Antonov, and O. Jepsen, *Thin Solid Films* **364**, 171 (2000).

¹⁶B. Lu, H. J. Zhang, H. Y. Li, S. N. Bao, P. He, and T. L. Hao, *Phys. Rev. B* **68**, 125410 (2003).

¹⁷H. J. Zhang, B. Lu, H. Y. Li, S. N. Bao, and P. He, *Surf. Sci.* **556**, 63 (2004).

¹⁸F. J. Himpsel, J. E. Ortega, G. J. Mankey, and R. F. Willis, *Adv. Phys.* **47**, 511 (1998).

- ¹⁹A. Pimpinelli and J. Villain, *Physics of Crystal Growth* (Cambridge University Press, Cambridge, 1998).
- ²⁰J. A. Venables, *Introduction to Surface and Thin Film Processes* (Cambridge University Press, New York, 2000).
- ²¹H. Brune, Surf. Sci. Rep. **31**, 121 (1998).
- ²²F. J. Meyer zu Heringdorf, M. C. Reuter, and R. M. Tromp, Nature (London) **412**, 517 (2001).
- ²³B. Voigtländer, Surf. Sci. Rep. **43**, 127 (2001), and references therein.
- ²⁴Z. Olami, Y. Manassen, N. R. Rao, and R. Dana, Surf. Sci. **520**, 35 (2002).
- ²⁵Y.-W. Mo, D. E. Savage, B. S. Swartzentruber, and M. G. Lagally, Phys. Rev. Lett. **65**, 1020 (1990).
- ²⁶B. Voigtländer and N. Theuerkauf, Surf. Sci. **461**, L575 (2000).